

AD-A184 238

DTIC
ELECTE
AUG 27 1987
S D
CED

DTIC FILE COPY (1)

ESL-TR-86-20

AIRCRAFT ENGINE EXHAUST PLUME DYNAMICS

B. TOD DELANEY
BRYAN A. ZETLEN
RONALD C. TAI
GLENN D. SEITCHEK
G. GREGORY ELCOCK

SCIENCE ENGINEERING
ASSOCIATES, INC.
701 DEXTER AVENUE, N, SUITE 400
SEATTLE WA 98109

DECEMBER 1984 - AUGUST 1985

FINAL REPORT

OCTOBER 1986

APPROVED FOR PUBLIC RELEASE: DISTRIBUTION UNLIMITED



ENGINEERING & SERVICES LABORATORY
AIR FORCE ENGINEERING & SERVICES CENTER
TYNDALL AIR FORCE BASE, FLORIDA 32403

87 8 21 055

NOTICE

PLEASE DO NOT REQUEST COPIES OF THIS REPORT FROM
HQ AFESC/RD (ENGINEERING AND SERVICES LABORATORY).
ADDITIONAL COPIES MAY BE PURCHASED FROM:

NATIONAL TECHNICAL INFORMATION SERVICE
5285 PORT ROYAL ROAD
SPRINGFIELD, VIRGINIA 22161

FEDERAL GOVERNMENT AGENCIES AND THEIR CONTRACTORS
REGISTERED WITH DEFENSE TECHNICAL INFORMATION CENTER
SHOULD DIRECT REQUESTS FOR COPIES OF THIS REPORT TO:

DEFENSE TECHNICAL INFORMATION CENTER
CAMERON STATION
ALEXANDRIA, VIRGINIA 22314

REPORT DOCUMENTATION PAGE

1a. REPORT SECURITY CLASSIFICATION UNCLASSIFIED			1b. RESTRICTIVE MARKINGS			
2a. SECURITY CLASSIFICATION AUTHORITY			3. DISTRIBUTION/AVAILABILITY OF REPORT Approved for Public Release Distribution Unlimited			
2b. DECLASSIFICATION/DOWNGRADING SCHEDULE			4. PERFORMING ORGANIZATION REPORT NUMBER(S)			
4. PERFORMING ORGANIZATION REPORT NUMBER(S)			5. MONITORING ORGANIZATION REPORT NUMBER(S) ESL-TR-86-20			
6a. NAME OF PERFORMING ORGANIZATION Science Engineering Associates, Inc.		6b. OFFICE SYMBOL (If applicable)	7a. NAME OF MONITORING ORGANIZATION HQ Air Force Engineering & Services Center			
6c. ADDRESS (City, State and ZIP Code) 701 Dexter Avenue, N, Suite 400 Seattle WA 98109			7b. ADDRESS (City, State and ZIP Code) HQ AFESC/RDVS Tyndall AFB FL 32403-6001			
8a. NAME OF FUNDING/SPONSORING ORGANIZATION Federal Aviation Administration		8b. OFFICE SYMBOL (If applicable) AEE-30	9. PROCUREMENT INSTRUMENT IDENTIFICATION NUMBER F08635-85-C-0036			
8c. ADDRESS (City, State and ZIP Code) 800 Independence Avenue, S.W. Washington DC 20591 Report #FAA-EE-86-8			10. SOURCE OF FUNDING NOS.			
11. TITLE (Include Security Classification) Aircraft Engine Exhaust Plume Dynamics			PROGRAM ELEMENT NO. 63723F	PROJECT NO. 2103	TASK NO. 9019	WORK UNIT NO.
12. PERSONAL AUTHOR(S) B. Tod Delaney, Bryan A. Zetlen, Ronald C. Tai, Glenn D. Seitchek, G. Gregory Elcock						
13a. TYPE OF REPORT Final		13b. TIME COVERED FROM Dec 84 to Aug 85		14. DATE OF REPORT (Yr., Mo., Day) October 1986		15. PAGE COUNT 27
16. SUPPLEMENTARY NOTATION Availability of this report is specified on reverse of front cover. Distribution notice--Destroy by any method that will prevent disclosure of contents or						
17. COSATI CODES			18. SUBJECT TERMS (Continue on reverse if necessary and identify by block number)			
FIELD	GROUP	SUB. GR.	Aircraft engine exhaust plumes reconstruction of			
20	13		Dispersion modeling this document.			
21	05		Pollution			
19. ABSTRACT (Continue on reverse if necessary and identify by block number) This report summarizes a research effort to remedy a known deficiency in the Air Quality Assessment Model dispersion calculation capability. Current methods use dispersion calculations and equations for vertical sources (i.e., power plants) resulting in inaccurate assumptions when applied to the horizontal source of an aircraft engine. This study examined the dispersion of aircraft engine exhaust by using infrared thermal imaging techniques. These results were compared to theoretical equations describing jet exhaust plumes. The resulting validation provided the necessary equations and support to mathematically model this phenomena.						
20. DISTRIBUTION/AVAILABILITY OF ABSTRACT UNCLASSIFIED/UNLIMITED <input checked="" type="checkbox"/> SAME AS RPT. <input type="checkbox"/> DTIC USERS <input type="checkbox"/>			21. ABSTRACT SECURITY CLASSIFICATION UNCLASSIFIED			
22a. NAME OF RESPONSIBLE INDIVIDUAL Lt GLENN D. SEITCHEK			22b. TELEPHONE NUMBER (Include Area Code) (904) 283-4234		22c. OFFICE SYMBOL RDVS	

UNCLASSIFIED

SECURITY CLASSIFICATION OF THIS PAGE

UNCLASSIFIED

SECURITY CLASSIFICATION OF THIS PAGE

PREFACE

This research was conducted by Science and Engineering Associates, Inc, 701 Dexter Avenue, N., Suite 400, Seattle WA 98109. It was conducted under contract number F08635-85-C-0036 and JON 21039019 for the Headquarters Air Force Engineering and Services Center, Research and Development Directorate, Environics Division, Tyndall AFB FL 32403-6001. Mr Don Silva and Mr Bryan Zetlen were the Principal Investigators, and Lt Glenn D. Seitchek was the AFESC Project Officer.

The work began in December 1984 and was completed in August 1985. This report covers the results of the project.

This report has been reviewed by the Public Affairs Office (PA) and is releasable to the National Technical Information Service (NTIS). At NTIS, it will be available to the general public, including foreign nationals.

This technical report has been reviewed and is approved for publication.

Glenn D. Seitchek
GLENN D. SEITCHEK, 1Lt, USAF
Project Officer

Kenneth T. Denbleyker
KENNETH T. DENBLEYKER, Maj, USAF
Chief, Environmental Sciences Branch

Robert F. Olfenbutte
ROBERT F. OLFENBUTTEE, Lt Col, USAF, BSC
Chief, Environics Division

James R. VanOrman
JAMES R. VAN ORMAN
Deputy Director of Engineering and
Services Laboratory

Accession For

NTIS CPA&I	<input checked="" type="checkbox"/>
DTIC TAB	<input type="checkbox"/>
Unannounced	<input type="checkbox"/>
Justification	

By _____
Date _____

Approved _____
Date _____

A-1

C. 411
INSP
2

TABLE OF CONTENTS

Section	Title	Page
I	INTRODUCTION.....	1
	A. OBJECTIVE.....	1
	B. BACKGROUND.....	1
	C. SCOPE.....	3
II	TEST APPROACH.....	5
	A. TEST EQUIPMENT AND SITE REQUIREMENTS.....	5
	B. TEST PROCEDURE.....	6
III	ANALYSIS.....	11
	A. JET ENGINE EXHAUST PLUME CHARACTERISTICS.....	11
	1. General Behavior.....	11
	2. Plume Stages.....	11
	3. Near-Wall Effect.....	12
	4. Vertical Instability.....	12
	B. THEORETICAL CONSIDERATIONS.....	12
	1. Background.....	12
	2. Free Jets.....	13
	3. Energy Dissipation in Turbulent Jets.....	15
	C. COMPARISON OF THEORETICAL CALCULATIONS WITH EXPERIMENTAL OBSERVATION.....	16
	1. Observed Versus Theoretical (Horizontal Jet Assumed)...	16
	2. Observed Versus Theoretical (Inclined Jet Assumed).....	16
	3. Turbulent Energy Considerations.....	19
	D. ADDITIONAL OBSERVATIONS.....	19
IV	CONCLUSIONS AND RECOMMENDATIONS	23
	A. TEST DATA CONCLUSIONS.....	23
	B. RECOMMENDED AUGMENTATION OF AQAM.....	23
	REFERENCES.....	27

LIST OF FIGURES

Figure	Title	Page
1	Landing Takeoff Cycle.....	2
2	Jet Plume Boundary Puffing.....	7
3	Plume Stages.....	11
4	Schematic Representation of Jet.....	14
5	Comparison of Experimental Observation with Horizontal Jet Plume (A-7).....	17
6	Comparison of Experimental Observation with Horizontal Jet Plume (A-6).....	18
7	Comparison of Experimental Observation with Inclined Jet Plume (A-7).....	20
8	Comparison of Experimental Observation with Inclined Jet Plume (A-6).....	21
9	Extent of Jet Plume Envelope by Engine Setting.....	25

LIST OF SYMBOLS

- A dimensionless coefficient approximately equal to 1
- B coefficient ranging from 1 - 10
- C Constant (0.081 assumed)
- D jet exit diameter
- ϵ_A energy dissipation rate in the atmosphere
- ϵ_j turbulent energy dissipation rate in a jet
- F engine thrust in pounds
- L_0 distance from jet exit at which jet velocity profile develops a Gaussian distribution
- μ_m micron
- ρ_e density of the fluid discharged
- σ standard deviation of velocity profile "x" distance from the jet exit
- u velocity in "x" direction
- u_{max} jet centerline velocity at distance "x" from jet exit
- U_0 jet exit velocity
- x axial distance from jet exit
- x_e distance from jet exit where the jet's turbulence dissipation rate equals that of the atmosphere
- z distance from jet centerline

SECTION I

INTRODUCTION

A. OBJECTIVE

The objective of this study was to enhance the predictive capability of the Air Force Air Quality Assessment Model (AQAM) through more accurate measurement and description of aircraft jet engine exhaust plume characteristics (size and pollutant concentration) by including momentum and thermal energy values in plume size calculations.

B. BACKGROUND

The importance of aircraft as a major source of visible air pollution has decreased over the last 20 years, especially since the introduction of clean engines in the latter part of the 1960s and early 1970s. However, the significance of aircraft as a source of reactive hydrocarbons and oxides of nitrogen has increased. This increase is attributable to today's flight environment which is characterized by intensified operations schedules (i.e., more flights than in the past) and the current generation of aircraft engines which produce considerably higher concentrations of oxides of nitrogen (at high power settings) than previous designs. Since these pollutants are primary constituents of photochemical smog, air pollution, as well as its dispersion from aircraft and airports, remains a significant issue.

An accurate environmental assessment of aircraft engine exhaust constituents has three primary components:

1. The measurement of pollution emissions to categorize them for each operational mode of each type engine.
2. Accurate descriptions of aircraft operational procedures to facilitate total released emission calculations.
3. An appropriate dispersion model to predict the resulting ambient air quality on which assessments of health and welfare effects are based.

Considerable development effort has gone into improving the calculation of the quantity and distribution of pollutants emitted by individual aircraft during the different events in the Landing and Takeoff (LTO) cycles (Figure 1).

LANDING TAKE-OFF CYCLE (LTO)

TAKE-OFF EVENTS

- Engine Start
- Taxi
- Engine Checks
- Take-off Roll
- Climb Out

LANDING EVENTS

- Approach
- Runway Rollout
- Taxi
- Idle/Shutdown

Figure 1. Landing Takeoff Cycle

Preliminary comparisons of predicted and measured ambient air concentrations made with AQAM have shown that the model predicts pollutant levels which generally withstand correlative analysis. However, this same analysis clearly indicates areas in which improvement is highly desirable. Discussion of the existing disparity between observed and predicted values centers on limitations in the current characterization of the background environment, (i.e., The model's failure to account for material transported into the sampling area from unknown sources or from sources within the airport or airbase which were not adequately modeled.)

Both current and experimental versions of AQAM, incorporating only rudimentary consideration of jet engine exhaust momentum and thermal energy, assume a relatively small plume size that is nonbuoyant and, thus, remains near the ground. Tank (Reference 7) has shown that jet engine exhaust thermal energy and momentum have a significant impact on the determination of plume dimensions for dispersion modeling. Further, Sprunger (Reference 6) has shown initial plume dimensions to be among the more sensitive input parameters in AQAM. These works serve as the basis for questioning the adequacy of current AQAM plume modeling as well as the inclusion of thermal energy and momentum in the proposed, refined description of plume behavior during engine start, taxi, and takeoff runway roll.

C. SCOPE

This program investigated, through infrared imaging, the development and dispersion of jet engine exhaust plumes produced by a variety of civilian and military aircraft and turbine engines. The tests were conducted over 7 months at several military and civilian airports.

SECTION II
TEST APPROACH

A. TEST EQUIPMENT AND SITE REQUIREMENTS

The principal objective of this program was to obtain visually discernible and quantifiable effects in jet engine exhaust plume development and dispersion.

A number of methods are available to study diffusion of turbojet plumes in the atmosphere including:

1. Introduction of oil or water into the exhaust plume to make it visible.
2. Use of temperature and velocity sensing arrays to delineate plume fringe.
3. Remote, noninvasive sensing techniques such as infrared (IR) imaging.

For this study, the IR imaging technique was chosen because of its success in previous test programs using static-mount and taxiing aircraft engines (Reference 4), its portability, and the spectral sensitivity required for accurate imaging. Plume growth and dispersion were measured by tracking jet exhaust products including water vapor (H_2O), carbon dioxide (CO_2), and carbon monoxide (CO) all of which exhibit vibration-rotation absorption bands in the middle IR spectrum (1.0 μm - 10 μm).

A review of appropriate, available test instrumentation was instituted at the outset of the program to establish both desired criteria and availability of equipment. The review established the following:

- visual imaging of plume effects, i.e., size, development, dispersion, vortices, etc. requires infrared sensitive (2-5 micron range) optical instrumentation; the ability to 'translate' this image via videoprocessing, into visible frequencies; and the memory capacity to store data for eventual reexamination and interpretation
- one-man portability and operation in the field (outdoors, runways, etc.) including sufficient operational endurance for extended test runs
- ancillary support: battery, generator, and 120 vac power
calibration equipment
cryogenic supplies and storage
video and photographic equipment
audio recording equipment

Suitable components and systems which met these criteria and were used in the test portion of the program include:

- o AGEMA Thermovision Model 750 with Polaroid

- o AGEMA Thermovision Model 782 with 7 degrees and 20 degrees field of view (FOV) and isotherm discrimination capability
- o I.S.I. Videotherm Model 91 (pyroelectric vidicon temperature differential based imaging)
- o INFRAMETRICS Model 600 Imaging Radiometer with video processor and false colorizer

Other systems reviewed and considered suitable for obtaining refined temperature data and smaller incremental temperature variations included:

- HUGHES Probeye Thermal Video Series 4000
- EVEREST Interscience Infrared Thermometers
- I.S.I. Model 86
- EG&G Photoradiometer
- C.I. Spectroradiometer SR 9000

B. TEST PROCEDURE

The test program was conducted by placing the IR sensing system perpendicular to the exhaust plume and from 50 to 300 feet downstream of the tail of the aircraft. The target aircraft would then run its engine at a number of different power settings including idle, slow and fast taxi, takeoff/military power and afterburner. During engine runup, and at each power setting, the point at which individual vortex and/or plume boundary layer disruptions and discontinuities appeared ("Puffing," as shown in Figure 2), meteorological data, and engine operating parameters were recorded on audiotape and written logs. If known measurement benchmarks were visible, actual plume measurements were taken during IR imaging. If such background comparitors were not readily available, measurements were later derived by analysis of known aircraft component measurements (i.e., tail height) and known distance of camera from plume. The puffing was characterized as to downstream distance and vertical development. The IR video was taped for later playback, additional processing, and analysis.

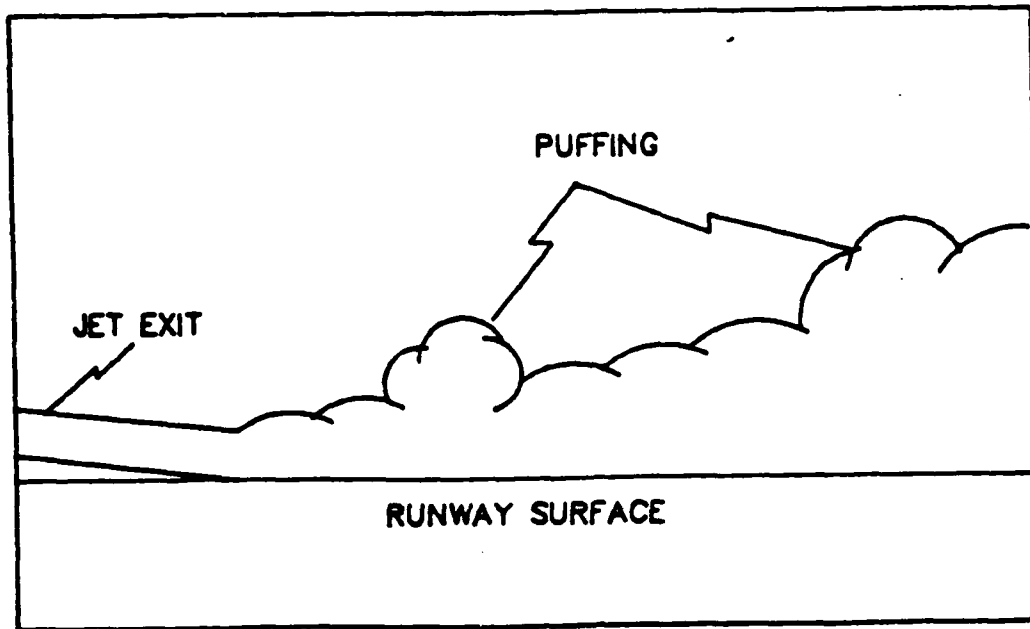


Figure 2. Jet Plume Boundary Puffing

At each test location, time-correlated meteorological data were taken from one or more of the following sources:

- portable meteorological tower
- base/airport weather station
- observable conditions at test sites, (i.e., compass headings, wind direction, etc.).

Local weather parameters (bounds) were established including the following criteria dictated by limitations of infrared imaging equipment and local disruptive effects such as heat point sources, background thermal noise sources, and relatively warm runways and taxiways:

- local air temperature less-than-or-equal to 70° F.
- little or no precipitation
- no fog (IR and runway safety considerations)
- variety of local stability values.

Orientation, scale and distance measurements were provided directly from aircraft specifications, (e.g., top of tail section to ground = 16 feet; exhaust outlet diameter = 18 inches, etc.) Physical measurements were taken of site landmarks, buildings, natural objects, and known benchmarks such as runway paving blocks. Compass readings were taken for directional orientation of winds, plume vectors, and instrumentation-to-aircraft angles. Typical test setups would consist of instrumentation positioned perpendicularly to the long axis of the tailpipe/plume at a distance of 75 feet to 200 feet from the aircraft.

Particular care was taken to minimize thermal noise interference by positioning test setups to avoid 'noisy' infrared emitting or reflecting sources such as mountains, dark buildings and point sources such as smokestacks, storage tanks, ground transport and power generators. Instruments were calibrated immediately before each test run to ensure that data were taken from identical infrared sensitivity baselines.

Engine types vary by model and on an individual basis with respect to output observable in the infrared. Different engines of the same type and model may vary considerably in outputs of H₂O vapor, CO₂, and particulates at various power settings. Uniformity of output was not required however, as the tests established that plume development and dispersion are not observably affected by species and particulate content.

Because of pilot endurance and runway operational considerations, static test runs were of no more than 30 minutes duration in which requests were transmitted by radio to pilot, or through tower for alterations in power settings.

For tests during LTO, instruments were positioned on runway and taxiway side aprons and were moved to coincide with and track the movement of aircraft. Voice recordings of observations were made on the videotapes recorded during the later phase of the test program. In addition to providing data on local conditions, the voice commentary allows for pinpoint synchronization of very rapid transient observables in the plumes.

Various means of isolating potentially significant effects in plume development included:

1. Isotherm focusing -

Utilization of the video/IR processor capability to isolate very narrow portions of the viewed image and to precisely determine the radiated temperature of that area.

2. Compressed-time (high-speed) imaging -

Running the video data tapes at faster than real-time speed produced enhanced images of transient plume effects.

3. Still photography of isolated plume events -

Attempts were made to utilize a polaroid photography mechanism provided on one of the infrared cameras to record transient plume effects. The results were unsatisfactory as it proved impossible to activate the mechanism rapidly enough to capture the brief phenomena.

4. False color separation

False color assignments by species type and relative temperature were made, and reverse (white/black) video were used during test runs to more accurately and precisely identify boundary vortices, "puffs," and other characteristics of plume development and dispersion.

5. Telescopic magnification

The loss of resolution and image detail caused by use of telescopic lenses outweighed their usefulness in enlarging images.

6. Pyroelectric-triggered vidicon imaging

Imaging by temperature differentials only, rather than by actual temperature and types of materials in the plume.

Exhaust plumes from a number of aircraft were examined. Those from which useful data were taken include:

Type:	Engine:
o A-7	TF-30
o EA6B	J52-P408
o A-6	J52-P8

additional data, although insufficient for complete analysis, were taken from:

o C9	JT8D
o 727	JT8D
o 737	JT8D-9
o T38	J85-5A
o F14	TF30-412A
o S3	TF34-400A
o C141	TF33-7
o F4	J79

To the maximum extent possible, these measurements were taken during those periods of the day which minimized the undesirable effects of runway, taxiway, and background heating. Plume behavior was recorded during both day and night periods and under varying conditions of wind, rain, and fog.

SECTION III

ANALYSIS

A. JET ENGINE EXHAUST PLUME CHARACTERISTICS

1. General Behavior

The general behavior of the jet engine exhaust plume of an aircraft can be described as similar to that of a hot turbulent air jet emitted from a round orifice near a plane solid surface, in a direction generally parallel to that surface, and into an air medium at ambient temperature. Depending upon the situation, the air medium may be stationary or moving at a mean flow speed and direction, independent of the jet flow. The theoretical derivation and experimental observation of such fluid flow systems has not been well established.

2. Plume Stages

The general characteristics of a high-speed air jet as it is emitted into a similar medium of different temperature can be described as occurring in three stages (Figure 3). In the initial stage, the jet turbulence and growth are dominated by the momentum of the exiting air due to its high velocity in relation to ambient. Typically, this distance is approximately 7 times the diameter of the exhaust port of the engine.

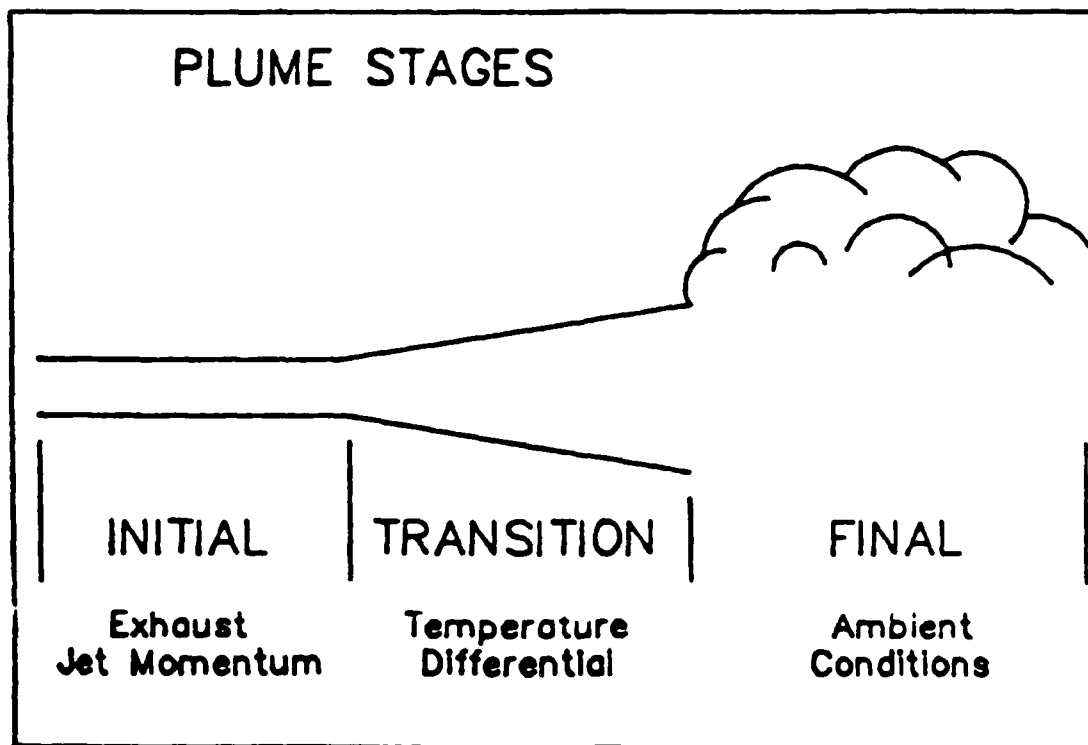


Figure 3. Plume Stages

The transition stage begins when temperature differences between ambient and internal jet air masses begin to affect the turbulence near the edge of the jet creating instability in the jet flow motion (i.e., the buoyant effect becomes more important). The final stage begins when, after a certain distance (dependent on engine thrust and ambient conditions, i.e., wind), both the thermal and momentum effects of the jet diminish to a degree where ambient conditions (wind speed and thermal stability) take over. This distance is a function of the initial jet temperature and velocity relative to ambient conditions. Jet plume growth after this final stage is totally dependent on ambient conditions and, as such, plume emissions can be viewed as imaginary point sources within the ambient environment.

3. Near Wall Effect

Another important factor determining the characteristics of the jet plume is the effect of a solid surface near the jet. Davis and Winarto (Reference 5), observing the overall effect of a wall near a jet, reported a flattening of the jet cross section in a direction perpendicular to the surface when compared with a free jet whose centerline paralleled the solid surface. However, in the case of many tactical military aircraft, the exhaust jet plume is often inclined at an angle towards the ground. In these instances, the interaction between the jet plume and the ground (solid surface) is further complicated. A thickening effect in the jet plume's vertical direction was anticipated due to boundary friction between the jet flow and the ground. This effect tends to counterbalance the flattening effect observed by Davis and Winarto (Reference 5). The precise behavior resulting from the interaction of these effects is not clear from existing, available studies.

4. Vertical Instability

The vertical instability of a jet plume as it proceeds farther from the exhaust nozzle has seldom been addressed in jet plume studies. Since the predominant mean air motion in the initial stage of a jet plume is generally horizontal, vertical plume development is not expected to deviate from that induced by the plume's mean turbulent motion until such time as the thermal energy in the plume overcomes this motion. The theoretical derivation of the governing relationship for this phenomena is not readily available though its presence may be indicated by the deviation of experimental observations from theoretically derived values as jet turbulence due to momentum begins to give way to thermal instability.

B. THEORETICAL CONSIDERATIONS

1. Background

The theoretical consideration in the present study deals primarily with the initial jet effect of the progressive stages mentioned above. Jet plume growth will be better illustrated through comparison of theoretical projections and field observation data. Since typical jet exit velocities are much higher than typical ambient winds, no attempt is made to consider the effect of crosswind on the plume motion. This assumption is based upon empirical observation and appears valid for the initial jet portion within a short distance from the jet exit (approximately 75 feet).

Brubaker et al. (Reference 3) attempted to describe the initial jet plume effect in terms of its centerline trajectory in a crosswind using empirical equations derived by Abramovich (Reference 1) and theoretical relationships derived by Briggs (Reference 2). The intent was to establish a virtual effective source location based on the lateral deflection of the jet plume. The horizontal deviation of an initial jet plume was considered and a crosswind was assumed.

2. Free Jets

The schematic description of a turbulent free circular jet (three dimensional, axially symmetric) is depicted in Figure 4 (next page) as a fluid discharged from a circular nozzle into a stationary medium of similar density. The initial velocity profile at the jet exit takes a finite distance, L_0 , to develop into a Gaussian type distribution. Beyond this point in the jet, the velocity profiles are assumed to be similar in nature for all free jets and can be expressed as:

$$\frac{u}{u_{\max}} = \exp\left(\frac{-z^2}{2\sigma^2}\right) \quad (1)$$

where u_{\max} is the centerline velocity at a given axial distance x , u is the velocity (in x direction) at a point z distance away from the centerline, and σ is the standard deviation of the velocity profile at distance x from jet exit.

For a given jet exit velocity, u_0 , the centerline velocity at any distance greater than L_0 can be expressed as:

$$\frac{u_{\max}}{u_0} = \frac{D}{2Cx} \quad (2)$$

where D is the jet diameter at the exit and C is experimentally determined and defined as:

$$\frac{\sigma}{x} = C \quad (3)$$

The constant C , depending on the literature cited, may range from 0.067 to 0.105. A commonly used value is 0.081. This reduces Equation (2) to:

$$\frac{u_{\max}}{u_0} = 6.2 \frac{D}{x} \quad (4)$$

The axial distance where jet flow will be fully established falls approximately $7D$ distance from the jet exit. The jet exit velocity can be related to the jet characteristics and jet engine operational condition as:

$$u_0 = \frac{2}{D} \left(\frac{F}{\pi \rho_e} \right)^{1/2} \quad (5)$$

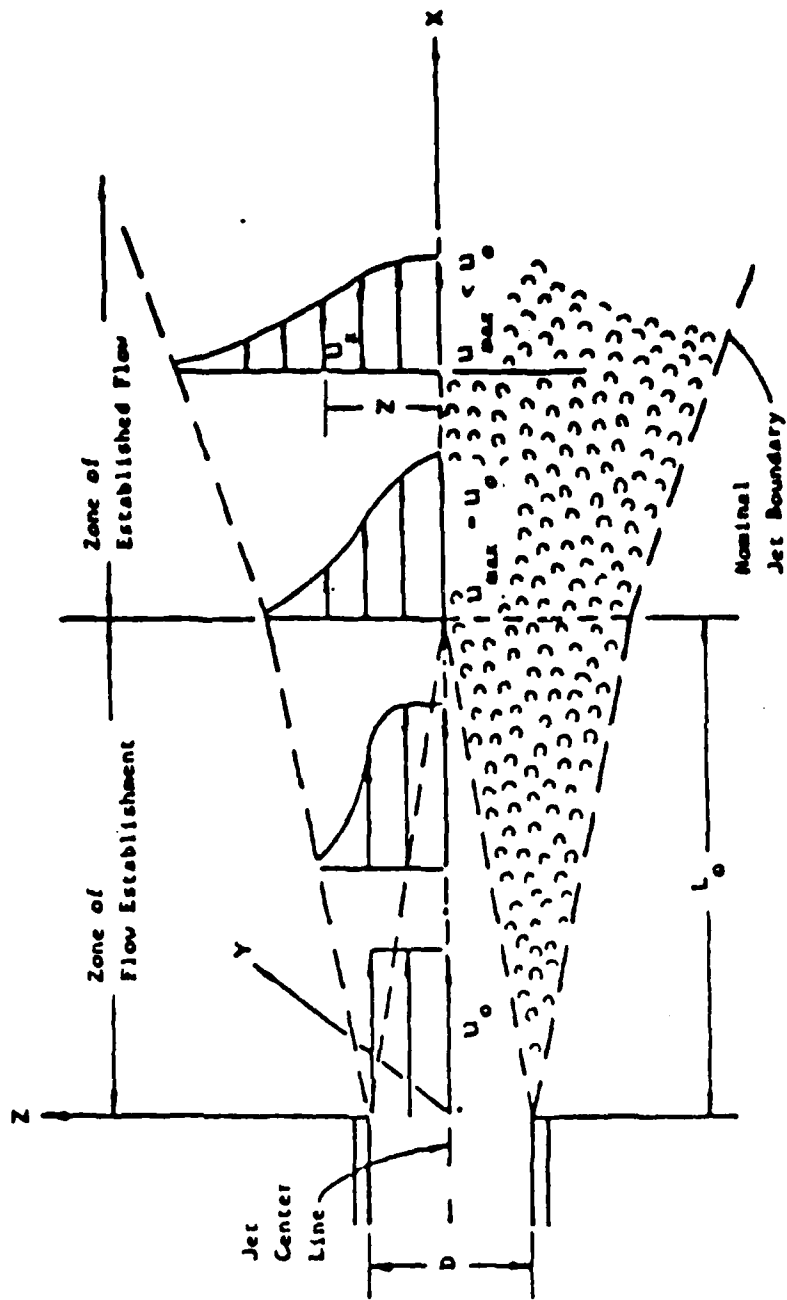


Figure 4. Schematic Representation of Jet

where F is the engine thrust and ρ_e the density of the fluid discharged.

The above equations provide a theoretical description of a well-developed jet which allows the combination of Equations (1), (2), and (4) to give:

$$z = 0.081 \left[2 \ln \left(6.2 \frac{u_0 D}{ux} \right) \right]^{1/2} \quad (6)$$

Equation (6) describes the velocity distribution at a series of points in a jet and may be used to calculate the profile of the plume boundary using the chosen envelope velocity defining the edge of a given jet. This particular application of the equation is useful in comparison with the experimental observations on the jet boundary under varied conditions.

3. Energy Dissipation in Turbulent Jets

Brubaker et al. (Reference 3) have derived a relationship quantifying the turbulent energy dissipation rate in a jet as in comparison with turbulent energy dissipation present under ambient conditions. This relationship has its basis in the original Tennekes and Lumley (Reference 8) definition of the energy dissipation rate in a jet.

$$\epsilon_j = A \frac{u_{max}^3}{\sigma} \quad (7)$$

where A is a dimensionless coefficient of the order of unity and ϵ_j is the turbulent energy dissipation rate in a jet.

Further, it was assumed that:

$$\epsilon_j = B \epsilon_A \quad (8)$$

where ϵ_A is the energy dissipation rate in the atmosphere and B is a coefficient ranging from 1 to 10. Applying Equations (3), (4), and (8) to Equation (7), Brubaker et al. arrived at the relationship that defines the distance from the jet exit where the jet turbulent energy dissipation rate equals that of the ambient atmosphere (i.e., $A/B = 1$).

For an observationally-based representative sample jet spread angle of 10.5 degrees, the relationship takes the form:

$$\frac{x_e}{U} = 7.3 \left(\frac{u_0^3}{D \epsilon_A} \right)^{1/4} \quad (9)$$

where x_e denotes the distance from the jet exit where the jet turbulence and ambient atmosphere dissipation rates are equal and provides an indication of the relative strength of the jet turbulence. It should be noted that actual jet flows are expected to deteriorate well before the calculated distance due to the influence of other factors such as thermal and ground effects.

C. COMPARISON OF THEORETICAL CALCULATIONS WITH EXPERIMENTAL OBSERVATIONS

1. Observed versus Theoretical (Horizontal Jet Assumed)

Equation (6) was used to predict the boundary of actual engine exhaust jet plumes from the jet exit point until the jet's linear mean velocity decreased to 50 miles per hour. The 50 mile-per-hour value was chosen after review of both USAF and civilian documents that delineated the routinely measurable safety exclusion zones for jet powered aircraft. Recorded data from field observations on military aircraft A-7 and A-6s were summarized and compared with the theoretical calculations as outlined above. Specific parameters for the aircraft are the exhaust pipe inside diameter (2 feet for the A-7 and 1.5 feet for the A-6), nozzle height above ground during level parking (3.5 feet for the A-7, and 6.1 feet for the A-6), and the corresponding range thrust level setting at idle (1000-1500 pounds for the A-7 and 1500-2000 pounds for the A-6). The A-7 is a single engine aircraft while the A-6 is a twin engine aircraft. The thrust range of 1500-2000 pounds for the A-6 was used as an approximate value for the combined effects of both engines at the idle thrust level. Figures 5 and 6 show Equation (6) derived plot of the jet plume boundary for the two thrust settings assuming the jet exited parallel to the ground for the A-7 and the A-6, respectively.

Figures 5 and 6 also show the jet plume boundary extracted from the experimental observation made by Davis and Winarto (Reference 5) for a jet near a solid flat surface. In the case of these tests, the wall effect is created by the ground. Davis and Winarto (Reference 5) have studied jet flow near a solid flat surface. The jet upper boundary above the surface was defined in their study as the location above the surface where the jet velocity is one half the maximum velocity (u_{max} in Figure 1) within the jet at a particular distance from the jet nozzle. Equation (6) was applied to this velocity definition of boundary. The resulting calculated upper boundary, as defined by Davis and Winarto using Equation (6), is independent of jet characteristics. Both the calculated boundary (Equation (6)) and the observed boundary extracted from the experimental data from Davis and Winarto are included in Figures 5 and 6 for reference. These curves are not suitable for direct comparison with the field observation from the current study. However, the one-half- u_{max} boundary comparison did confirm the flattening effect of the flat surface on a jet flow nearby.

Observed plume boundary limits, as shown in Figures 5 and 6, reveal consistently well-defined plume boundaries close to the jet exit point and puffing, nonlinear degradation of the defined boundary at distances of 60 to 90 feet for the A-7 and 130 to 150 feet for the A-6. This degradation may indicate plume breakdown occurring, at least in the plume boundary regions. It can also be seen that the theoretical ideal jet, as presented here for both aircraft types, tends to overpredict the jet plume thickness as compared with the experimental data in the near range and underestimate it in the far range.

2. Observed versus Theoretical (Inclined Jet Assumed)

Figures 7 and 8 illustrate the comparison of the same observations as above (A-7 and A-6 aircraft) with the theoretical results (based on identical input parameters as used in Equation (6)) of free jet boundaries whose axes

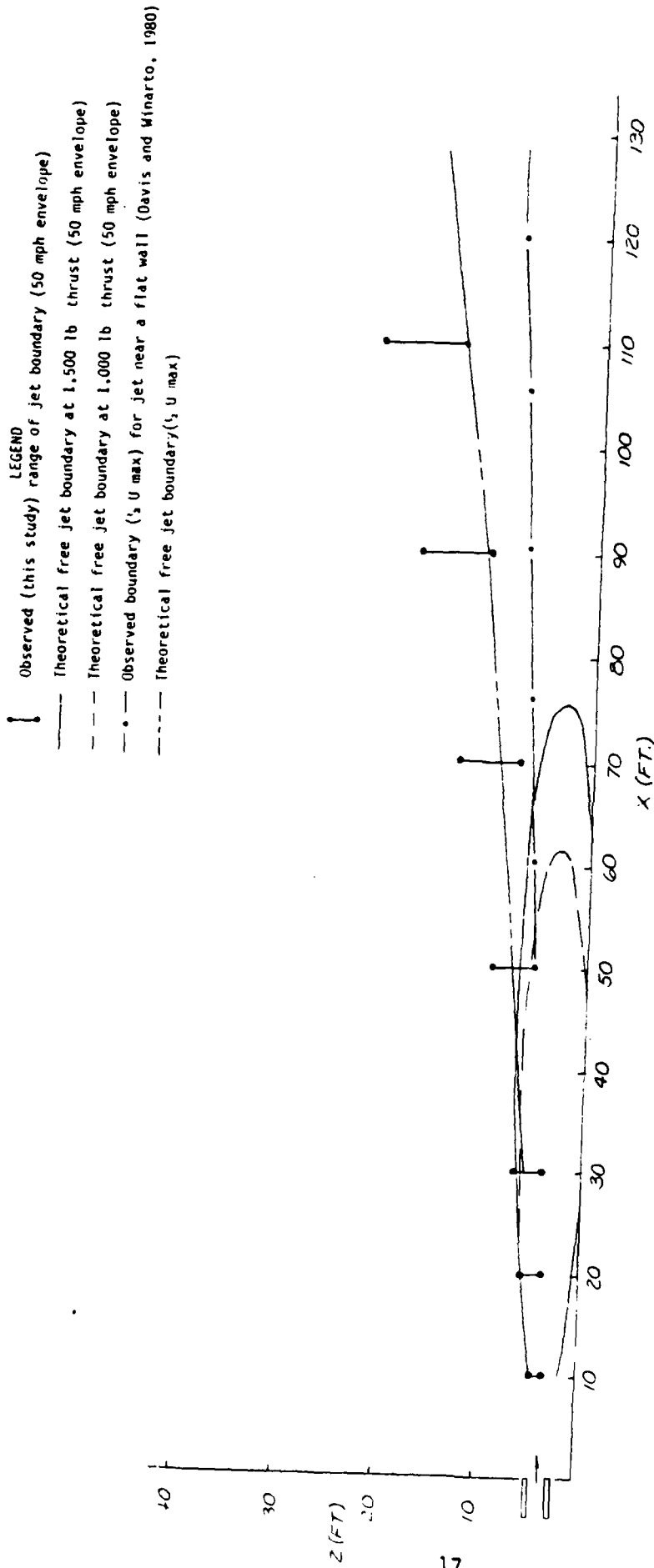
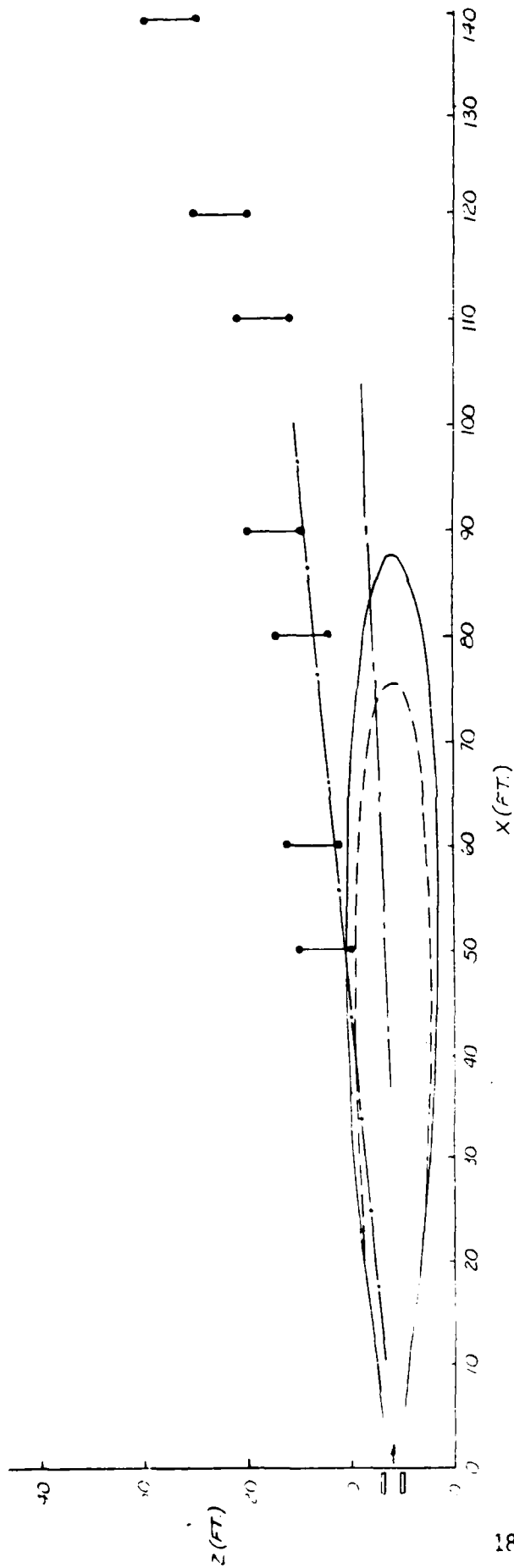


Figure 5. Comparison of Experimental Observation with Horizontal Jet Plume (A-7)



LEGEND

- observed (this study) range of jet boundary (50 mph envelope)
- - - - theoretical free jet boundary at 2,000 lb thrust (50 mph envelope)
- - - - theoretical free jet boundary at 1,500 lb thrust (50 mph envelope)
- · - · - observed boundary (U_{max}) for jet near a flat wall (Davis and Minarto, 1980)
- · · · theoretical free jet boundary (U_{max})

Figure 6. Comparison of Experimental Observation with Horizontal Jet Plume (A-6)

were inclined 5 and 10 degrees from the horizontal for the A-7 and 10 and 15 degrees for the A-6. These jet angles more closely represent the actual conditions under which the experimental data were collected. In each case the jet plume centerline reaches ground level within a short distance of the jet nozzle and is assumed to be "perfectly" reflected from the ground (e.g., no frictional or other losses). Within short "x" distances, the characteristics and magnitude of the theoretical jet boundary fall within the range of observed jet plume boundaries.

As shown in Figures 7 and 8, differences between observed and theoretical plume boundary location increase at distances beyond 60 feet from the jet nozzle. After this point in the jet stream (approximately 50-60 feet for the A-7 and 90-100 feet for the A-6 from tailpipe), the momentum of turbulent flow is expected to play a progressively less important role in the plume's growth as the thermal effect becomes more pronounced.

3. Turbulent Energy Considerations

Equation (9) estimates the location in a jet plume where the turbulent energy dissipation rate is equal to that experienced in ambient air. For a neutral stability atmosphere, the energy dissipation rate ϵ_A carries a value of 0.125 (Reference 3). By inserting the parameters employed in jet flow calculation, Equation (9) yields equivalent jet and ambient dissipation rates at a distance of 2,000 feet from the jet nozzle. This distance, well beyond the observed location where jet boundary instability begins, indicates jet momentum predominance diminishes well before the turbulent energy dissipation in the jet approaches that of the ambient atmosphere. Even for unstable atmospheric conditions, it is expected that the jet plume Gaussian dispersion effect would become more significant a substantial distance before "turbulent equilibrium."

The thickening of the plume in the vertical dimension can likely be attributed to thermal instability overcoming jet momentum in combination with increased frictional interaction between the jet flow and the solid boundary. Typical of similar fluid flows, puffing of the jet plume results from increased convective mixing with ambient air and the presence of turbulent eddies on a larger scale. Field observations position actual jet plume puffing coincident, or nearly so, along the horizontal axis with the theoretically derived limits of the jet plume boundaries.

D. ADDITIONAL OBSERVATIONS

Test conditions (meteorological, instrumentation type, distances and orientation) where data were taken from aircraft other than A-7s and A-6s approximated those prevailing during the A-7 and A-6 test runs. The principal difference in data obtained from the second group of aircraft is in quantity. These aircraft were filmed as occasional targets of opportunity and the test team had neither control over nor knowledge of power settings. Therefore, no specific conclusions can be drawn from the data with the exception of information regarding plume geometry, time and distance characterization of plume development, and dispersion. Since no duplicate data or control existed over test condition parameters during filming of the targets of opportunity, specific quantification/prediction cannot be made for plume effects generated by the second group of aircraft.

- LEGEND
- Observed (this study) range of jet boundary (50 mph envelope)
 - ▨ Theoretical jet boundary range for 1,000 to 1,500 lb. thrust (50 mph envelope) for 5° jet inclined angle
 - ▭ Theoretical jet boundary range for 1,000 to 1,500 lb. thrust (50 mph envelope) for 10° jet inclined angle

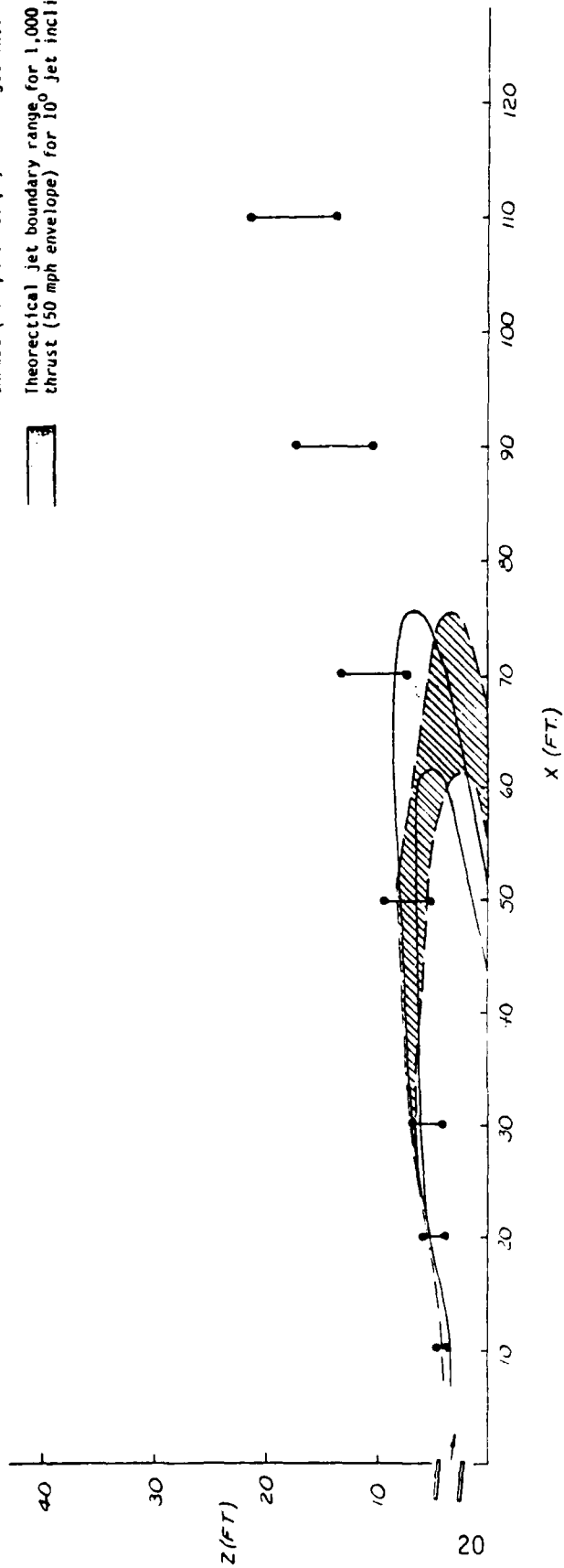


Figure 7. Comparison of Experimental Observation with Inclined Jet Plume (A-7)

LEGEND

- | Observed (this study) range of jet boundary (50 mph envelope)
- ▨ Theoretical jet boundary range for 1,500 to 2,000 lb. thrust (50 mph envelope) for 10° jet inclined angle
- ▭ Theoretical jet boundary range for 1,500 to 2,000 lb. thrust (50 mph envelope) for 15° jet inclined angle

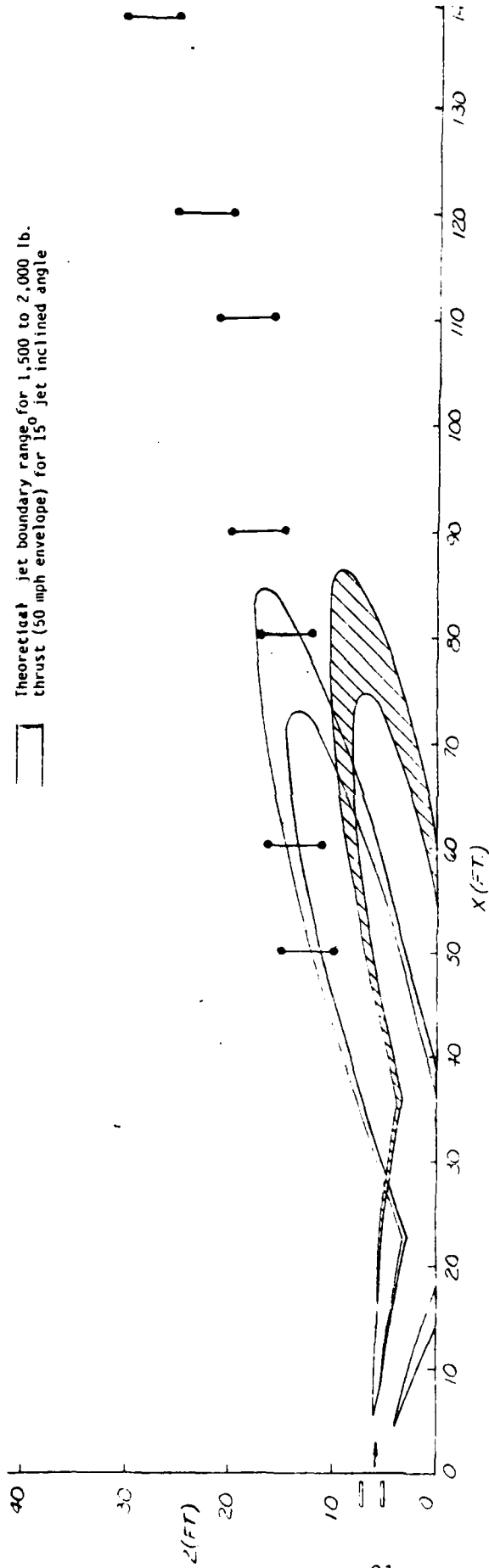


Figure 8. Comparison of Experimental Observation with Inclined Jet Plume (A-6)

For aircraft powered by medium or high bypass jets, for example, reengined 727s and 737s, and the S3 (Viking), the IR equipment lacked the sensitivity to adequately image these exhaust plumes which are much cooler than those produced by the zero- or low-bypass engines such as those on the A7 or older commercial and military aircraft. It was possible to view the thermal point sources but, at distances of greater than 3-4 meters from the exhaust, the exhaust plumes were no longer visible in the IR. Since physical laws govern the propulsive requirements of thrust-to-lift-and-weight ratios, it can safely be assumed that medium and high bypass engines do produce exhaust plumes similar to the lower bypass engines but the sensitivity and range of the available test equipment could not provide useful images of these events.

The respective angles of the horizontal axes of the engines on various aircraft produced a range of effects on the bodies of the plumes. These ranged from barely detectable heating of runways and taxiways beneath the engines to a marked disruption of the bodies of the plumes. Since these effects were generally tangential to the horizontal axis and direction of flow, these rebound phenomena were similar in appearance but more sharply defined than those effects generated at the boundary layer interface.

The combination of low resolution/sensitivity in the IR equipment, rapid development and dispersion and temperature 'normalization' of plume puffs to ambient temperature often required extreme concentration and repeated examination of the video data. This problem was effectively resolved by running and viewing the videotapes at increased speed producing sharper images and enhanced contrast of the puffs against the thermal background. It was also useful to employ the 'false' color capability of the IR color processor to assign arbitrary color to temperature and species constituents of the plume images to further increase observability of thermal differences and changes in the plume/ambient interface.

With the observed exception of wind velocities exceeding 20 mph (particularly at angles approaching perpendicular or opposite to the plume flow), local stability Categories A through F and transitions between stability levels had no observable effect on plume development or dispersion.

The eddy and vortex effects occurring along the boundary layer drew ambient, therefore, cooler air into the plume. These actions contributed to a more moderate vertical plume growth than might otherwise be expected. The locations of these eddies also helped define the plume boundaries.

Potential data collection deficiencies and errors may occur as a function of limitations in the IR sensitivity of the cameras used in these tests. For example, if plume temperature fell below the sensitivity threshold of the equipment yet was still greater than ambient temperature, it is possible that plume momentum relative to ambient was sustained for distances greater than those observed during these tests.

SECTION IV

CONCLUSIONS AND RECOMMENDATIONS

A. TEST DATA CONCLUSIONS

Pertinent theoretical and experimental studies on free jet flow and jet flow near a solid surface have been reviewed. Appropriate information was extracted from these reports and applied to and/or compared with present experimental observations and calculations. The comparisons indicated that an idealized, ground reflected jet plume seems to fit best, both qualitatively and quantitatively, the observed jet plume boundary ranges.

The present study found jet plume size to be a function of engine power setting and other characteristics, i.e., the diameter of the jet exit, the angle of the jet's axial flow in relation to the runway/taxiway. Examination of current data revealed initial plume dimensions to Gaussian dispersion of $6D$ and $13D$ (thickness and width, respectively) at a distance of 60-90 feet from the jet exit of the A-7. These compare favorably with the $8D$ and $10D$ dimensions observed by Chen (Reference 4) from a T-33. In both studies, observed plume dimensions were significantly larger than those assumed in current AQAM applications. Sprunger's work (Reference 6), having found initial plume dimension to be one of the more sensitive AQAM input parameters, supports the recommendation that the idealized, ground-reflected jet developed in this study be incorporated into the AQAM modeling process.

B. RECOMMENDED AUGMENTATION OF AQAM

It was determined that plume momentum persistence was, to a substantial degree, a function of engine thrust and power setting. In instances of twin engine aircraft, the combined thrust of centerline-mounted engines acted to produce plume momentum persistence approximately equivalent to that which would be produced by a single engine of thrust equal to that produced by the combined center-mounted engines. It was also observed that twin- and multiengine aircraft with wing-mounted or otherwise non-centerline-mounted engines produced discrete plumes having development and dispersion characteristics appropriate to their individual thrust ratings and power setting.

The extent of the 50 mph plume envelope and its characteristic changes with the engine thrust setting are of significant interest from the perspective of considering the initial condition for the jet exhaust plume dispersion process. Figure 9 illustrates the theoretical curve as calculated using Equation 6, as well as the theoretical curves adjusted to fit the respective observed location of the initial jet plume at approximately idle setting for the two aircraft types studied.

These two curves can be employed to determine the approximate distance for the onset of atmospheric dominated plume growth for all power settings except afterburner. The curve, labeled single engine, would be typical for aircraft having a single engine or multiengines that are separated by considerable distances, while the curve labeled twin engine should be used for

aircraft that have twin engines or when the engines are relatively close together. Thus, these curves can be employed to determine the approximate distance as a function of the thrust setting for single or multiple engine aircraft. Once this distance has been determined the initial size of the plume can be defined as a function of the exhaust nozzle diameter. The current study supports previous findings that at idle conditions the exhaust dimensions are in the range of 6 to 8 times the diameter of the jet exit in height and 10 to 13 times the diameter in width for a single engine aircraft.

The corresponding values for plume height for dual engine aircraft as developed in this study are 9 to 12 times the diameter of the jet exit. Sufficient observations were not available to provide an estimate of the width, but one could assume that on a similarity basis the width would be on the order of 1.5 times the single engine value or a value of 15 to 20 times the diameter of the jet exit.

The procedures that have been proposed here for use in AQAM are intended to provide a reasonable means of estimating the distance, height and width of the plume at the probable location that atmospheric condition will dominate. These procedures will provide approximate numbers that are representative of the actual conditions. Consequently, they should be employed with the knowledge that they are best estimates based on field observations and theoretical calculations.

LEGEND

- Theoretical (Equation 6)
- A7 aircraft at idle (single engine, 1000 lb thrust)
- E68 aircraft at idle (twin engine, 1000 lb. thrust each)
- Expected range based on A7 and E68 data

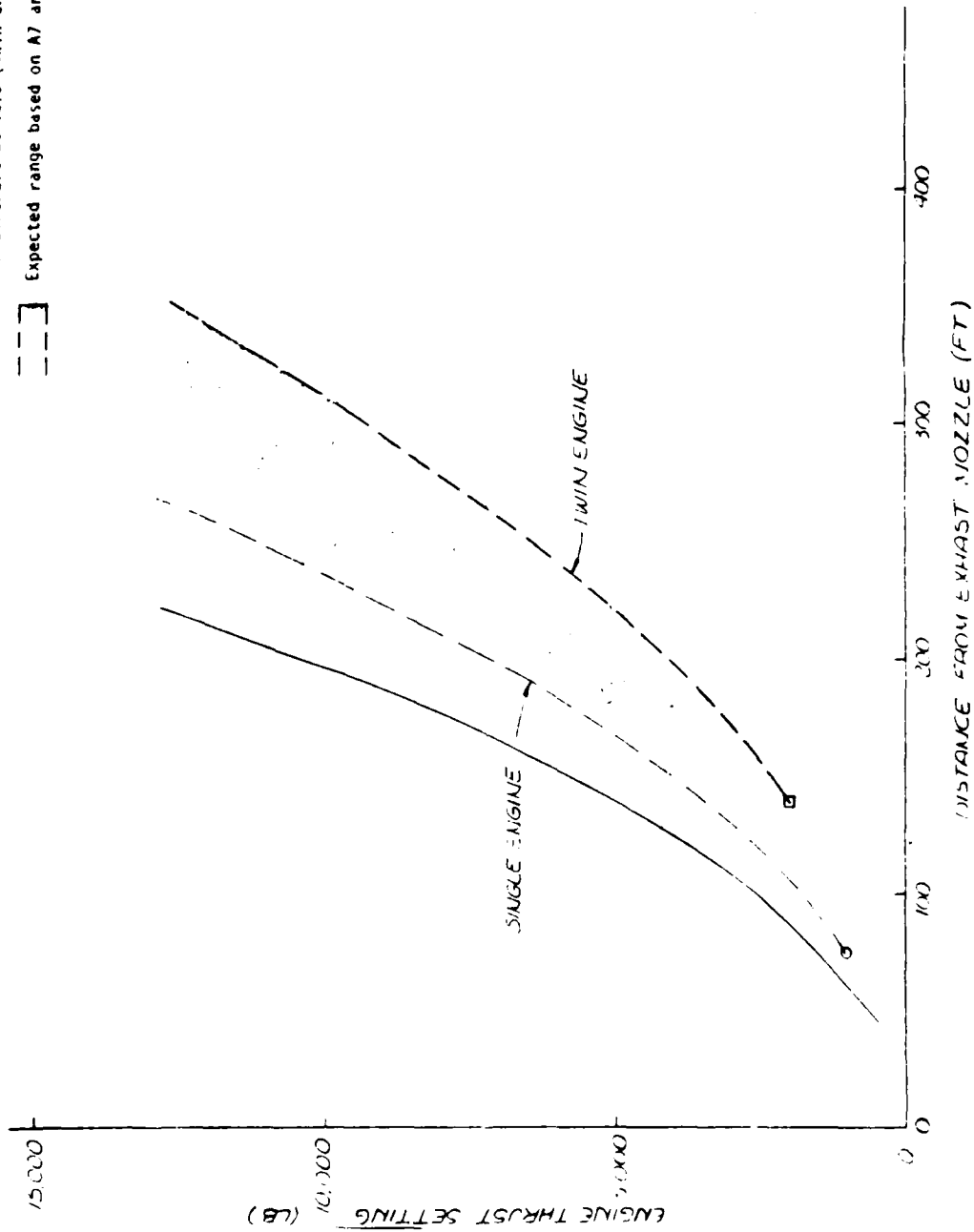


Figure 9. Extent of Jet Plume Envelope by Engine Setting

REFERENCES

1. Abramovich, G. N., The Theory of Turbulent Jets, The MIT Press, Cambridge, MA, 1963.
2. Briggs, G. A., Plume Rise Predictions in D. A. Hanqar, ed., Lectures on Air Pollution and Environmental Impact Analysis, American Meteorological Society, Boston, MA, 1975.
3. Brubaker, K. L.; Dave, M.; Wingender, R. J.; and Flotard, R. D., Impact of Aircraft Emissions on Air Quality in the Vicinity of Airports, Volume IV: Nitrogen Oxide and Hydrocarbons, FAA-EE-84-14 Argonne National Laboratory, Argonne, IL, 1984.
4. Chen, A. T., Engine Exhaust Plume Growth Geometry. Document No. D6-49298TN. Boeing Commercial Airplane Company, Seattle, WA, 1980.
5. Davis, M. R.; Winarto, H., "Jet Diffusion from a Circular Nozzle above a Solid Plane," J. Fluid Mech. 101:201-221, 1980.
6. Sprunger, R. R.; Wangen, L. E., Numerical Studies on the Errors in Model Parameters, Argonne National Laboratory, Argonne, IL, 1975.
7. Tank, W. G.; Air Quality Workbook Final Report; Document Number D6-48742, Boeing Commercial Airplane Company, Seattle, WA, August 1979.
8. Tennekes H. and Lumley J.I., First Course in Turbulence, MIT Press, Cambridge MA, 1972.